Available online at www.sciencedirect.com
SCIENCE DIRECT®
Tetrahedron 60 (2004) 7225–7235
Tetrahedron

ROMP of *t*-butyl-substituted ferrocenophanes affords soluble conjugated polymers that contain ferrocene moieties in the backbone

Richard W. Heo, Joon-Seo Park, Jason T. Goodson, Gil C. Claudio, Mitsuru Takenaga, Thomas A. Albright and T. Randall Lee*

Department of Chemistry, University of Houston, 4800 Calhoun Road, Houston, TX 77204-5003, USA

Received 17 April 2004; revised 7 June 2004; accepted 14 June 2004

Available online 8 July 2004

Abstract—A substituted ferrocenophane, 1,1′-((1-*tert*-butyl)-1,3-butadienylene)ferrocene, was synthesized and polymerized via ring-opening metathesis polymerization (ROMP) to give soluble high molecular weight polymers with ferrocenylene units in the backbone. The monomer readily underwent polymerization upon exposure to a tungsten-based metathesis initiator, W(=CHC$_6$H$_4$-*o*-OMe)(=NPh)[OCMe(CF$_3$)$_2$]$_2$ (THF), to give high molecular weight polymers (M_w=ca. 300,000). The molecular weights could be varied systematically by adjusting the monomer-to-catalyst ratio. UV/vis spectra revealed a bathochromic shift for the polymer, consistent with enhanced conjugation compared to the monomer. The polymer exhibited thermal properties similar to oligomeric poly(ferrocenylene). Cyclic voltammetry of the polymer suggested that the iron centers are coupled electronically. Upon doping with I_2 vapor, the polymers displayed semiconducting properties (σ=10^{-5} S cm^{-1}). Theoretical calculations were used to evaluate the nature of the bonding in these and related polymers.

1. Introduction

Conjugated polymers have been widely studied because of their potential use as lightweight and flexible substitutes for metals in a variety of applications.[1–13] Materials based on conjugated polymers function as conductors of electricity because of electron delocalization through their planar π-system. Interest in conjugated polymers that contain transition metal backbones has been sparked by the promise of a new class of material that will combine the attractive electrical properties of metals with the strength, flexibility, and processability of organic polymers.[6] Previous attempts, however, to synthesize 'organometallic' polymers have typically afforded poorly conducting and poorly soluble oligomeric materials that are of dubious practical use.[14,15] The planar π-system that gives conjugated polymers their desired electrical conductivities also causes them to be intractable and infusible. These latter characteristics contribute to a decrease in mechanical strength and processability, which have slowed the incorporation of conjugated polymers in device applications. Sensitivity to ambient conditions (e.g. oxygen, heat, and light) has also limited the widespread use of conjugated polymers. Overcoming these limitations will be necessary before conjugated polymers will be of practical utility in all but highly specialized technologies.

In an effort to generate a new type of conjugated material, we are exploring the development of organometallic polymers that will be both (1) good conductors of electricity and (2) readily soluble in common organic solvents. Our strategy, which has been reported in preliminary form,[16,17] involves the synthesis of specifically designed ferrocene-containing monomers that undergo facile polymerization to yield conjugated polymers that contain ferrocenyl units in the polymer backbone. Ferrocenes are attractive building blocks for conjugated polymers for at least three reasons: (1) the ferrocene linkages can act as rotatable π−π-bonds,[18] lending solubility (and thus processability) to the resultant materials, (2) the functionalization of ferrocenes has been well developed, offering a variety of substituted ferrocene-based monomers for the purpose of generating chemically and structurally well-defined ferrocene-containing polymers,[19] and (3) the remarkable air stability and thermal stability (>500 °C) of ferrocenes can be expected to lend enhanced stability to the resultant polymers.[20]

A wide variety of ferrocene-based organometallic polymers are known. In one particularly successful system,

Keywords: Ring-opening metathesis polymerization (ROMP); Soluble conjugated polymers; Ferrocenophane.
* Corresponding author. Tel.: +1-713-743-2724; fax: +1-281-754-4445; e-mail address: trlee@uh.edu

0040–4020/$ - see front matter © 2004 Elsevier Ltd. All rights reserved.
doi:10.1016/j.tet.2004.06.067

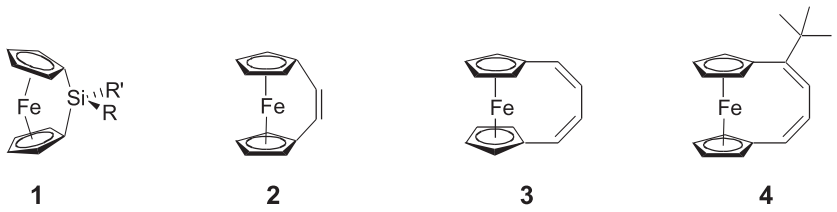

Figure 1. Selected ferrocenophane monomers used in various polymerization trials.

[1]ferrocenophanes bridged by heteroatoms such as germanium, silicon, and phosphorus (e.g. **1** in Fig. 1) have been synthesized.[21–27] The strain in these ferrocenophanes serves as a destabilizing factor, which leads to facile thermal ring-opening polymerization (ROP).[24–28] This strategy can be used to generate ferrocene-based materials possessing high molecular weights. The high molecular weight polymers are readily soluble when specifically designed solubilizing functional groups are incorporated in the monomers. Although high molecular weight poly (ferrocenylsilanes) are insulating (σ=10^{-14} S cm^{-1}), amorphous samples act as weak semiconductors (σ=10^{-8} to 10^{-7} S cm^{-1}) upon doping with I_2.[14,24] These values of conductivity, however, are still lower than those reported for well known π-conjugated organic polymers, such as polyacetylene (σ=10^{5} S cm^{-1})[29] and poly(phenylenevinylene) (σ=10^{3} S cm^{-1}).[30] It is believed that upon polymerization, the heteroatoms lack the necessary π-overlap to afford high electrical conductivities. It is our belief that electronic conjugation would be optimized by incorporating π-conjugated organic spacers between the ferrocene units. Electronic conjugation through the M(d π) of ferrocene and (p π) of the organic spacers would be optimized to give higher electronic conductivity values. The increased conductivity along with the attractive properties afforded by ferrocene should lead to soluble conducting polymers with attractive thermal and air stabilities.

Previous attempts have been made to synthesize highly conjugated ferrocene-based polymers.[12,13,16,17,31–37] In one study particularly relevant to our work, Tilley and co-workers synthesized *ansa*-(vinylene)[2]ferrocenophane (**2** in Fig. 1) in moderate yield from the McMurry coupling of 1,1′-ferrocenedicarbaldehyde.[31] The highly strained molecule **2** was targeted as a monomer for ring opening metathesis polymerization (ROMP) to give poly(ferrocenylenevinylene). Indeed, the polymerization using a molybdenum-based ROMP initiator[38] yielded poly(ferrocenylenevinylene). However, due to its poor solubility, characterization of this conjugated oligomer was limited. Prior to the work involving **2**, 1,4-(1,1′-ferrocenediyl)-1,3-butadiene (**3** in Fig. 1) was explored as a precursor for the synthesis of poly(ferrocenylenedivinylene) via ROMP.[32] Similarly, this polymerization strategy afforded oligomers that were poorly soluble in organic solvents.

In our research,[16,17] we have adopted this latter type of strategy, but we have modified the monomer structure in efforts to enhance the solubility of the resultant polymers. We believed that judicious structural modification could lend enhanced solubility to conjugated polymers. Since the attachment of alkyl groups to the backbones of polymer chains is known to afford organic-soluble polymers,[39–41] we have designed versions of the monomer with a single alkyl substituent attached to the olefinic bridge (see **4** in Fig. 1). For example, the attachment of bulky pendant alkyl chains to rigid backbones has been shown to increase the solubility of poly(phenylenevinylene),[42] poly(*p*-phenylene),[43] and polypyrrole.[44] Similarly, substituted polyacetylenes produced from the ROMP of monosubstituted cyclooctatetraenes are soluble in organic solvents when the substituents consist of bulky alkyl groups.[39] Furthermore, the incorporation of polar functional groups has permitted the synthesis of water-soluble versions of polythiophene[40] and polyaniline.[41] When we initially undertook this strategy, we believed that the ROMP of bridge-alkylated derivatives would afford readily soluble versions of polymer. We wished to enhance the solubility in order to facilitate polymer synthesis, characterization, evaluation, and manipulation (i.e. processing).

At least four factors motivated us to choose ROMP as the methodology for synthesizing conjugated organometallic polymers. First, ROMP conserves the number of double bonds (i.e. the degree of unsaturation) of the monomer upon its conversion to the polymer (see Scheme 1), which is a useful feature for the synthesis of conjugated materials. Second, the molecular weight distribution of ROMP-derived polymers is typically narrow, permitting the synthesis of conjugated polymers having well-defined conjugation lengths.[45–47] Third, certain ROMP initiators can tolerate a wide range of chemical functionalities and reaction conditions,[48] permitting the incorporation of functional groups that can be used to tune the electrical properties of conjugated polymers. Finally, ROMP can be used to prepare block copolymers having specific segments and/or end group compositions.[49,50] Based on a previous report of the ROMP of 1,4-(1,1′-ferrocenediyl)-1,3-butadiene **3**,[32] we chose the highly reactive tungsten-based metathesis initiator, W(=CHC$_6$H$_4$-*o*-OMe)(=NPh)[OCMe(CF$_3$)$_2$]$_2$(THF),[51] (see Scheme 1) as the ROMP initiator in the studies reported here.

2. Results and discussion

2.1. Synthetic approach

Scheme 2 highlights our strategy for preparing unsaturated alkyl-substituted ferrocenophanes. The cornerstone of our approach is the butenone-bridged ferrocenophane **9** first synthesized by Pudelski and Callstrom.[52,53] We targeted

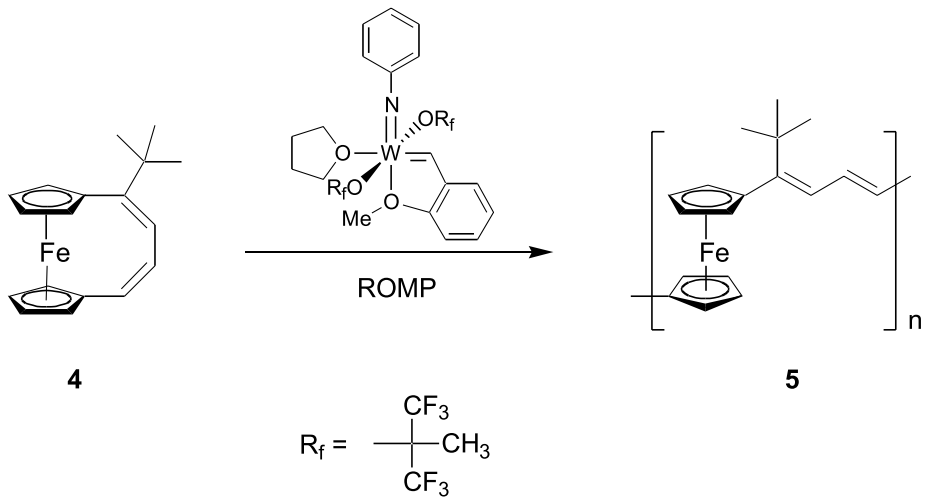

Scheme 1. ROMP of **4** gives *tert*-butyl substituted poly(ferrocenylenedivinylene) **5**.

carbon-1 (C-1) on the bridge of **9** as the site for the attachment of a pendant alkyl group. This strategy requires the use of an alkylating agent having no α-hydrogens, since the subsequent dehydration step will thus be restricted to form an endocyclic rather than an exocyclic double bond; the latter would likely predominate if α-hydrogens were available.[54]

2.2. Synthesis of 1,1′-((1-*tert*-butyl)-1,3-butadienylene)ferrocene 4

As illustrated in Scheme 2, alkylation at the C-1 position of **9** was achieved by the use of *tert*-butyllithium. Ferrocenophane **4** was synthesized successfully in two steps from 1,1′-(4-oxo-1-butenylene)ferrocene **9** in 43% overall yield. The crude product was purified by column chromatography followed by recrystallization from hexanes to give large orange needles of **4** that are stable in air and soluble in common organic solvents such as hexane, benzene, methylene chloride, toluene, and tetrahydrofuran (THF).

2.3. X-ray diffraction of 1,1′-((1-*tert*-butyl)-1,3-butadienylene)ferrocene 4

Although the single crystal X-ray structure of **4** has been reported,[16] we wish to highlight here certain structural features that illustrate the influence of the bulky substituent on the strain and consequent reactivity of **4**. The two Cp rings of **4** lie in a nearly eclipsed conformation and are almost parallel to each other. In contrast, the Cp groups of the parent unsubstituted 1,4-(1,1′-ferrocenediyl)-1,3-butadiene **3** (shown in Fig. 1) and the methoxy-substituted 1,1′-(1-methoxy-1,3-butadienylene)ferrocene **8** (shown in Scheme 2) lie in a staggered conformation and are substantially more tilted than those of **4**.[53,55] Moreover, the torsion angle of the butadiene bridge of the parent compound **3** is substantially larger (~42°) than that in **4** (~2°), further suggesting a relatively constrained geometry for **4**. Apparently, the steric bulk of the *tert*-butyl group gives rise to this constrained geometry, given that the smaller methoxy group in **8** exerts no similar effect. Concrete evidence of strain in **4** is most readily apparent

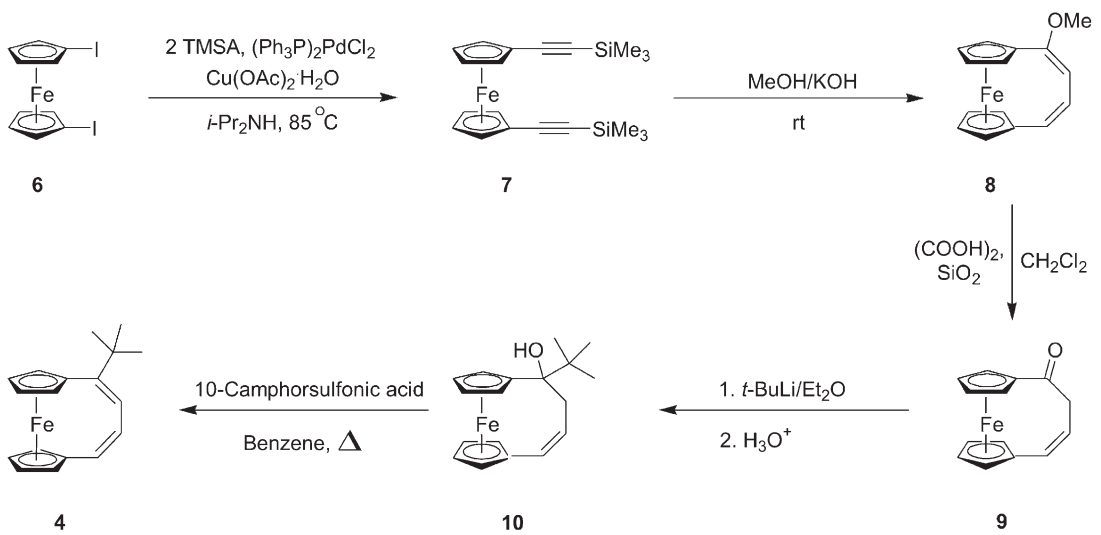

Scheme 2. Synthesis of 1,1′-((1-*tert*-butyl)-1,3-butadienylene)ferrocene **4**.[53]

Table 1. Comparison of the solubility of selected olefinic ferrocenylene polymers

Compound	Benzene	CH_2Cl_2	Toluene	THF
Poly(acetylene)[a]	×	×	×	×
Poly(ferrocenylene divinylene)[b]	×	×	×	×
Poly(ferrocenylene *tert*-butyldivinylene) **5**[c]	√	√	√	√

[a] From Ref. 15.
[b] From Ref. 32.
[c] From the present study.

as bond-angle strain in the sp^2 hybridized carbon atoms of the bridge, where the average C–C–C bond angle is 133°.[16]

2.4. Polymerization of 1,1′-((1-*tert*-butyl)-1,3-butadienylene)ferrocene 4

The strained structure of **4**, when coupled with the increased solubility afforded by the incorporation of the *tert*-butyl group, suggested to us that **4** should be a viable candidate for ROMP. Indeed, as shown in Scheme 1, ferrocenophane **4** readily undergoes ROMP to give the conjugated polymer **5**.[16,17] The polymerization was monitored in situ both visually and by ^{1}H NMR spectroscopy (see Fig. 2). Visible color and viscosity changes were detected in the polymer/catalyst solutions with time: the initially orange monomeric solution turned deep red and became more viscous as the reaction proceeded. As illustrated in Figure 2, analysis by ^{1}H NMR spectroscopy showed the disappearance of the sharp olefinic resonances at δ 5.82 and 6.37, and the appearance of broader olefinic resonances at δ 6.33, 7.03, and 7.68, respectively.

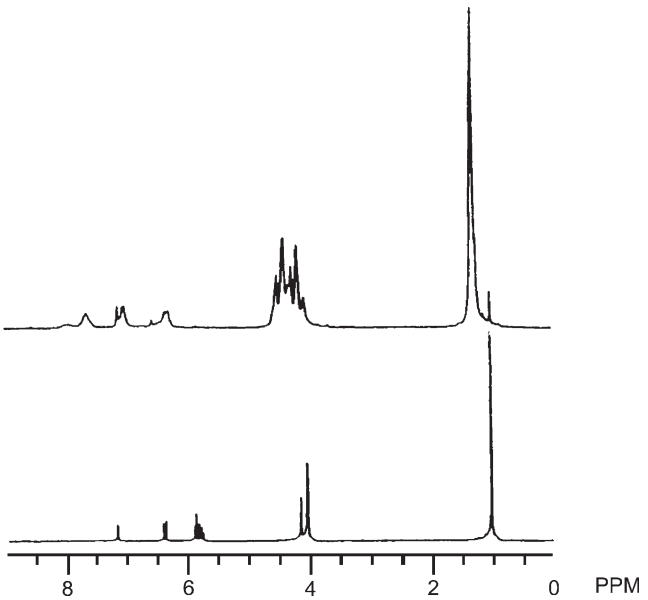

Figure 2. ^{1}H NMR spectra in C_6D_6 of the monomer **4** (lower) and its nearly complete ROMP to yield polymer **5** (upper).

The polymerization was terminated by the addition of benzaldehyde, which cleaves the polymer chain from the metal center.[32] The polymer was purified by precipitation into methanol and then repeatedly into hexanes from CH_2Cl_2 until the solution containing the precipitate became clear (typically 4 precipitations into hexanes). These steps serve to narrow the molecular weight distribution by removing trace amounts of unreacted monomer and low molecular weight oligomers. After reprecipitation, the overall yields of purified high molecular weight polymer were typically 60%. In the formation of high polymer, the lack of quantitative conversion coupled with the observation of low molecular weight oligomers suggests that the polymerization proceeds by a combination of living and nonliving polymerization mechanisms.[56] Removal of the solvent gave polymers that were stable to the atmosphere and could be stored for months under ambient conditions without detectable degradation. Polymers having $M_w \leq 100{,}000$ are brittle, while those with $M_w \geq 300{,}000$ are flexible, and can be readily peeled from glass slides. It is also noteworthy that these polymers are soluble in most common organic solvents (Table 1), which is rare for conjugated organometallic polymers having high molecular weights.[15]

Molecular weights of the polymer were measured by gel permeation chromatography (GPC) using THF as the eluant. Several polymerization trials were attempted to vary the molecular weights of the polymer by controlling the ratio of monomer to catalyst. The data in Figure 3 show that the molecular weights increase qualitatively as the ratio is increased, indicating that a moderate degree of control over the molecular weight can be achieved using this approach. We note further that the values of the polydispersity index are moderately low and fall within a narrow range (1.57–2.34). Importantly, the high molecular weights obtained here are unprecedented for soluble conjugated polymers with ferrocenylene units in the backbone, and rare for conjugated organometallic polymers as a whole.[14,15]

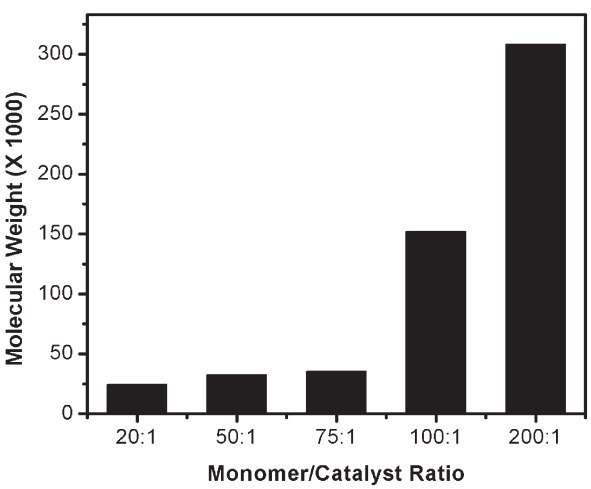

Figure 3. Molecular weight of polymer **5** as a function of monomer/catalyst ratio.

2.5. Spectroscopic characterization of monomer 4 and polymer 5

2.5.1. Analysis of the ^{1}H and ^{13}C NMR spectra. As shown in Figure 2, the ^{1}H NMR spectra of monomer **4** and the corresponding polymer **5** exhibit changes consistent with polymerization. Upon polymerization, for example, the ^{1}H NMR resonances become broader and shift downfield. The downfield shifts are consistent with an increase in electron delocalization for the polymer relative to the monomer.[42]

To a first approximation, the chemical shift difference between the H_α and H_β protons attached to the Cp rings of ferrocenophanes can be used to predict qualitatively the tilt of the Cp ring planes relative to each other.[21,24,31] Consequently, analysis of the chemical shifts of the Cp hydrogens in the ^{1}H NMR spectrum of **4** can be used to provide an indirect measure of the ferrocenophane ring strain arising from non-coplanarity of the Cp rings.[21,24,31] In the nonbridged 1,1′-divinylferrocene, for example, the difference between these chemical shifts is 0.18 ppm.[24] In the highly tilted *ansa*-(vinylene)ferrocene **2**, however, the separation is 0.79 ppm.[24] In contrast, the separation in monomer **4** is 0.11 ppm, which is consistent with little or no strain. While this interpretation is supported by the X-ray crystallographic data,[16] we reiterate that there is strong evidence of bond-angle strain in the sp^2 hybridized carbon atoms of the bridge of **4** (vide supra).

The ^{13}C NMR spectra of monomer **4** and the corresponding polymer **5** exhibited primary resonances consistent with their proposed structures (Fig. 4). Monomer **4** and crude polymer **5** displayed resonances between δ 65 and 75 arising from the carbons of the cyclopentadienyl (Cp) rings. The resonances associated with the corresponding carbons on polymer **5** were shifted slightly downfield and broadened compared to those of the monomer. For monomer **4**, the resonances associated with the olefinic carbons were observed between δ 125 and 130; for polymer **5**, these peaks were also broadened and shifted downfield relative to those of the monomer. The appearance of several resonances in the δ 120 region of the spectrum for polymer **5** is consistent with the presence of repeat units other than butadienes. Assuming that metal-mediated metathesis takes place solely at the unsubstituted double bond of **4**,[39,57] we believe a random combination of head-to-tail (see Scheme 1) and head-to-head/tail-to-tail polymerization mechanisms gives rise to the various olefinic carbon species. In our terminology, the head-to-head mechanism would afford ferrocene groups linked by a single unsubstituted olefin (Fc-CH═CH-Fc), and the tail-to-tail mechanism would afford ferrocene groups separated by a tri-olefin in which the *tert*-butyl groups are separated in a sequence of Fc-C (*t*-Bu)═CH–CH═CH–CH═C(*t*-Bu)-Fc.

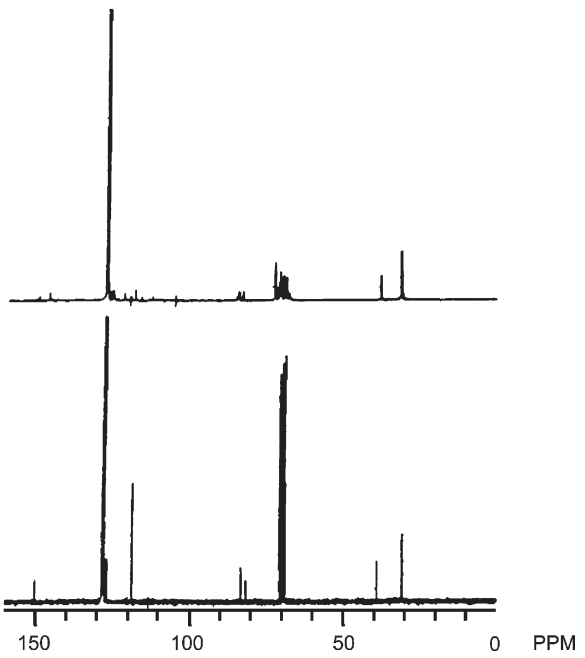

Figure 4. ^{13}C NMR spectra in C_6D_6 of the monomer **4** (lower) and polymer **5** (upper).

2.5.2. Ultraviolet/visible spectra. We measured the UV/vis spectra of both **4** and **5** in the range of 300–600 nm to examine the degree of electron delocalization in polymer **5** (See Fig. 5). As shown in the X-ray single crystal structure,[16] for monomer **4**, the π-orbitals in the bridge are perpendicular to those of the Cp groups, which significantly reduces conjugation. The polymer **5**, however, can adopt a conformation in which the π-orbitals in the bridge are nearly parallel to those of the Cp rings; thus, extended overlap between two sets of π-orbitals is possible. As noted above, visual inspection revealed that the solution turned from orange to deep red during the polymerization. Correspondingly, analysis of the UV/vis spectra for **4** and **5** revealed a bathochromic shift of λ_{max} upon polymerization characteristic of absorptions due to π to π* transitions of ethylenic chromophores: λ_{max} for **4**=444 nm; λ_{max} for **5**=472 nm (Fig. 5). Furthermore, while the monomer exhibited moderately intense absorptions (ε=4.5×10^3 M^{-1} cm^{-1}), the polymeric samples showed stronger absorptions (ε=1.2×10^4 M^{-1} cm^{-1}). These results are consistent with a moderate degree of conjugation for polymer **5**.[58]

It has also been shown that bathochromic shifts of the λ_{max} value of ferrocenophanes with respect to that of ferrocene reflect the degree of Cp-ring tilt (and thus ring strain) of the

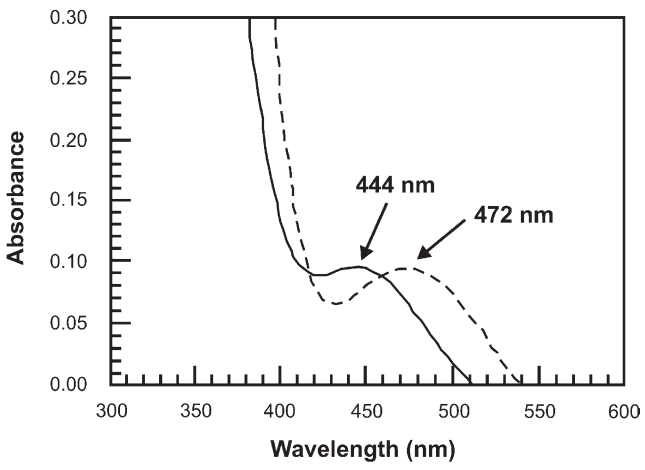

Figure 5. UV/vis spectra of monomer **4** (—, 2.1×10^{-4} M) and polymer **5** (- - -, 5.8×10^{-5} M).

former.[22] For example, Tilley's *ansa*-(vinylene)ferrocene **2** has a λ_{max} value (470 nm) that is red-shifted from that of ferrocene (440 nm);[31] this red shift is consistent with a substantial degree of ring tilt.[24,31] In contrast, however, our monomer **4** in which the Cp rings are nearly coplanar, displays a λ_{max} value of 444 nm—an absorption that is red-shifted with respect to that of ferrocene but less so than that of Tilley's monomer **2**. Consequently, given the known Cp ring tilts of the ferrocenophane monomers as determined by X-ray crystallography, the relationships outlined here are also consistent with the predicted relationship between the λ_{max} values and the relative Cp-ring tilts of ferrocenophanes.[24]

2.6. Thermal analysis of polymer 5

2.6.1. Thermal gravimetric analysis (TGA) of polymer 5. Examination of polymer **5** ($M_w \approx 240{,}000$) by TGA showed onsets of degradation at ca. 100 and 300 °C with substantial mass loss occurring above 550 °C (Fig. 6). The degree of thermal stability observed for this polymer is consistent with that reported for the structurally similar oligomeric poly (ferrocenylenebutenylene).[32] The thermal stability of polymer **5** is also comparable to other conjugated polymers in their undoped-states.[59] For example, polyacetylene, the simplest and most studied conjugated polymer, was shown by Ito and co-workers to be stable up to 300 °C in an inert atmosphere.[60] Moreover, poly(*p*-phenylene) was shown to be stable up to 400 °C in air and 550 °C in an inert atmosphere.[61] The thermal stability of polymer **5** reported here suggests that these new materials might find use in materials for solar energy conversion, organic semiconductors, and batteries where elevated temperatures are routinely encountered.[7]

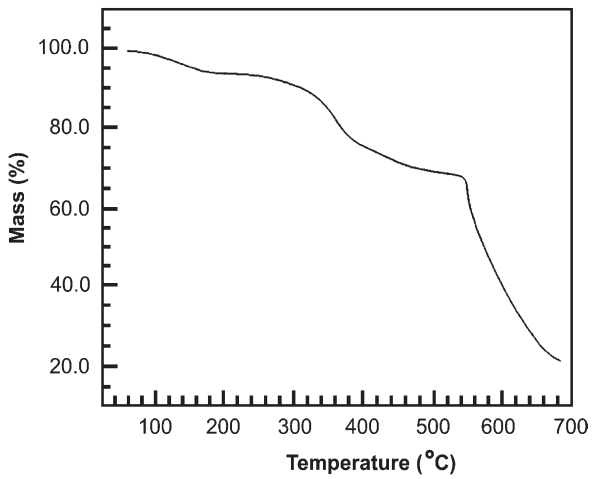

Figure 6. TGA plot for polymer **5** obtained under nitrogen.

2.6.2. Differential scanning calorimetry (DSC) of polymer 5. Examination of polymer **5** ($M_w \approx 240{,}000$) by DSC showed an endothermic transition at 65 °C followed by a large exothermic transition at 110–120 °C (Fig. 7). By analogy to the thermal characterization of aryl-linked poly(ferrocenylenes),[34] it is possible that the observed exothermic transition arises from a recrystallization process. Furthermore, the observed endothermic transition occurs at a temperature similar to that found for the endothermic

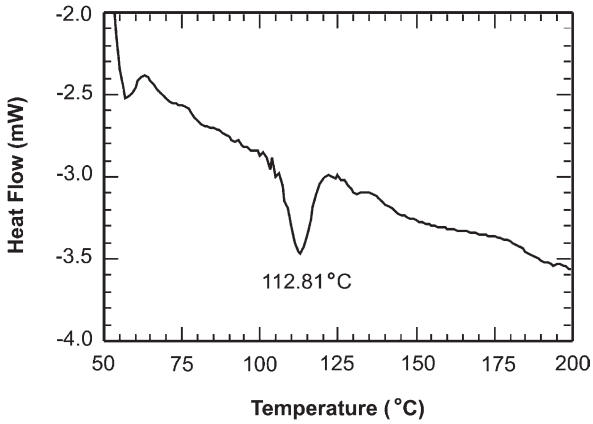

Figure 7. DSC plot for polymer **5** obtained under nitrogen.

transitions of structurally related derivatives of poly(1,1′-ferrocenylene-alt-*p*-oligophenylene).[34] We were unable to compare our data with that of the structurally similar oligomeric poly(ferrocenylenevinylene) because no DSC data were reported.[31] However, analysis by DSC of oligomeric poly(ferrocenylenebutenylene) reported no heat flow change until 385 °C.[32] Given that thermal phase behavior can be strongly influenced by (1) the degree of crystallinity and (2) minor physical variations such as small differences in molecular weight and/or the length of side chains,[34] it is unsurprising that distinct heat flow characteristics were observed for *tert*-butyl-substituted polymer **5** when compared to the unsubstituted parent oligomer.

The presence of aromatic moieties in conjugated polymer chains has been correlated with increased chain stiffness, T_g, and decomposition temperature.[59] Rehahn, and co-workers explored the thermal phase behavior of poly(1,1′-ferrocenylene-alt-*p*-oligophenylene) derivatives and the poly[2,9-(*o*-phenanthroline)-alt-*p*-oligophenylenes], which possesses no ferrocene moieties along the backbone.[34] While the latter polymers exhibit an endothermic transition at 190 °C, the former ferrocene-containing polymers, which are structurally related to our polymer **5**, show strong endothermic transitions at either 65 °C (*n*-dodecyl side chains) or 110 °C (*n*-hexyl side chains). It is possible that the reduction from 190 °C can be attributed to the considerably enhanced conformational freedom of the ferrocene-containing polymers.[34]

2.7. Electrochemistry

We performed electrochemical measurements of 1 mM CH_2Cl_2 solutions of ferrocene, the unsubstituted ferrocenophane **3**, the *tert*-butyl substituted ferrocenophane **4**, and the ROMP-generated polymer **5** (see Fig. 8). Tetrabutylammonium hexafluorophosphate (TBAHFP) was used as the electrolyte in these experiments in which the data were collected at a scan rate of 200 mV s^{-1} and the electrochemical potentials are reported relative to the standard calomel electrode (SCE). The cyclic voltammetry (CV) of solutions of ferrocene yielded a peak-to-peak separation of ~85 mV. The electrochemistry of ferrocene, **3**, and **4** were completely reversible between potentials of 0.00 and +1.00 V using the stated acquisition parameters. The measured electrochemical potentials for both **3** and **4** were

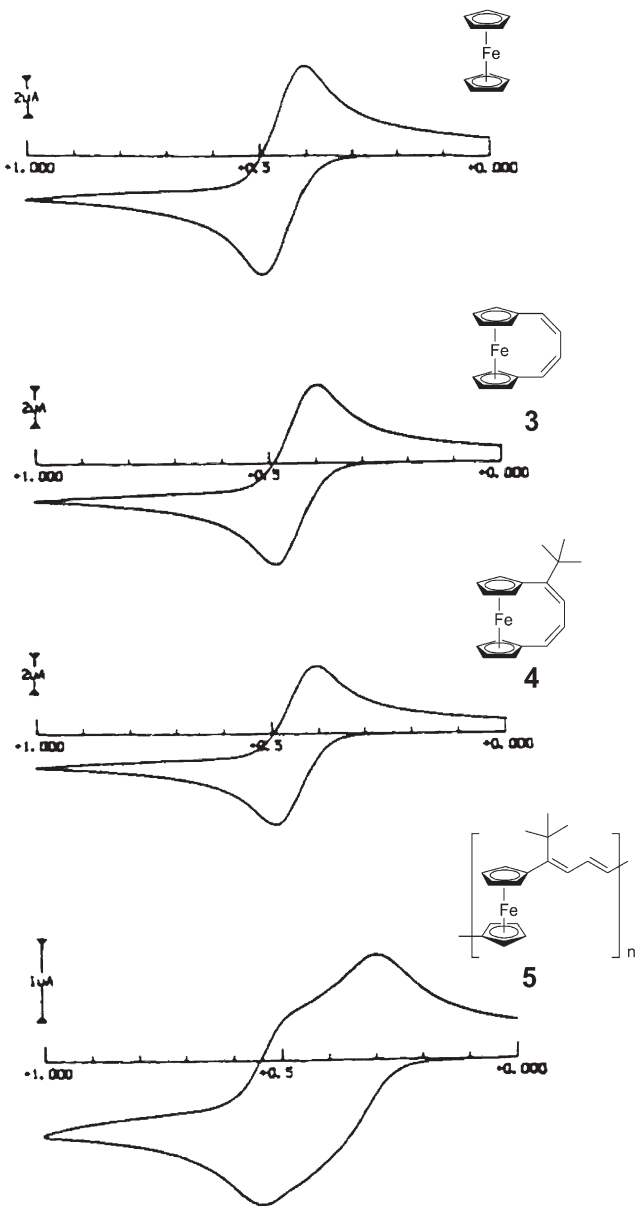

Figure 8. Cyclic voltammograms of 1 mM solutions of ferrocene, **3**, **4**, and **5** in 0.1 M TBAHFP-CH_2Cl_2.

E°=0.45 V, which is comparable to that measured for ferrocene (E°=0.44 V). Thus, the electrochemical potentials of the monomers were indistinguishable and within experimental error of that of ferrocene. These observations indicate that the presence of the four-carbon bridge (and alkyl substituents on the bridge) fail to influence the electrochemical potential of the ferrocene center. This conclusion is also supported by the ratio of anodic peak current to the cathodic peak current of the molecules. For example, at a scan rate of 200 mV s^{-1}, the ratio of anodic peak current to cathodic peak current was measured to be 0.96 and 0.99 for ferrocene and **4**, respectively.

Electrochemical methods were further used to probe the interaction between the iron centers in **5** (see Fig. 8). The redox waves for the polymer are reversible with a separation (ΔE) of 230 mV (M_w≈240,000, PDI=2.2). There was no apparent difference in redox properties found for polymers of low molecular weight vs. those of high molecular weight. The oxidation of the first electron in the polymeric system has a lower oxidation potential than that found for monomer **4** and, as expected, the removal of the second electron is more difficult than the first. The two-wave pattern and the magnitude of ΔE are characteristic of a chain possessing interacting metal centers.[62,63] Indeed, polymers having non-interacting centers would be expected to show only a single wave.[64] For example, saturated-hydrocarbon bridged [2]ferrocenophane were found to undergo ROP at high temperatures to give poly(ferrocenylethylenes).[65] Due to the more insulating characteristics of the saturated-hydrocarbon, the electrochemistry of poly(ferrocenylethylenes) showed the presence of only a single reversible oxidation wave, which indicates that the ferrocene groups interact to a lesser extent than in our polymer **5**. Furthermore, the observed magnitude of ΔE is comparable to that found for related ferrocenyl polymers that exhibit electronic communication between the iron centers, such as poly(ferrocenylenevinylene) (ΔE=250 mV)[33] and the heteroatomic polymers reported by Manners (ΔE∼210–290 mV).[24] Unfortunately, no data for poly(ferrocenylenedivinylene) were available due to the insolubility of the polymers and the lack of integrity of the polymer films during the collection of cyclic voltammograms in CH_3CN solutions.[32]

2.8. Doping and conductivity

Spin-coated samples of polymer **5**, which were highly resistive before doping (10^{11} Ω), were dried under vacuum on a Schlenk line equipped with an attachment for introducing I_2 vapor. After drying, the samples were treated with ca. 200 mm Hg of I_2 at ambient temperature. Instantly, the red translucent films became black. The films were exposed to vacuum for 30 min to ensure the removal of excess I_2 vapor from both the chamber and the film. The conductivity was measured with respect to the doping time as described in the Section 4. Films of polymer **5** (M_w≈240,000) that were treated in this manner exhibited maximum conductivities on the order of 10^{-5} S cm^{-1} (Fig. 9).

The measured conductivity of **5** is lower than that reported for either poly(ferrocenylenevinylene) (10^{-3} S cm^{-1})[31] or poly (ferrocenylenedivinylene) (10^{-4} S cm^{-1}).[32] Incorporation of

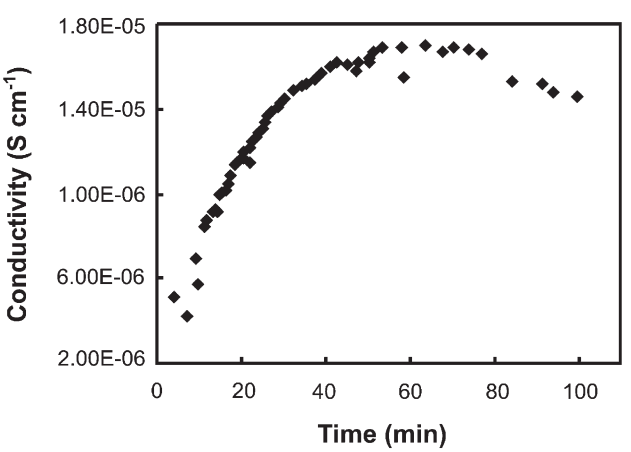

Figure 9. Vacuum conductivity of **5** as a function of the duration of exposure to I_2.

the sterically demanding *tert*-butyl group might plausibly lower the conductivity of **5**. Studies have shown, for example, that the introduction of a *tert*-butyl moiety along the backbone of polyacetylene causes a twisting from planarity of the chain, which partially interrupts the π-conjugation and thereby lowers the conductivity.[39] It is also possible that the steric bulk of the *tert*-butyl group lowers the conductivity via an alternative mechanism. If, for example, the major contributing pathway of electronic conduction in these polymers is due to interchain hopping rather than intrachain conduction via the polymer backbone, the bulky *tert*-butyl group might serve to hinder closest packing of the polymer chains and thereby inhibit hole transport.[39] Alternatively, the relatively low conductivity observed for **5** might be due to experimental artifact arising from differences in laboratory doping procedures and/or the manner in which the conductivity data were collected (e.g. the use of I_2-treated pressed pellets of the unsubstituted poly(ferrocenylenedivinylene)[32] vs. I_2-treated spin-coated films of **5**). On the whole, however, the data reported here provide further support that conjugated polymers with π-electron delocalization through ferrocenyl units are poorer electrical conductors than structurally related conjugated organic polymers such as poly(phenylenevinylene) (σ=10^3 S cm^{-1}).[30]

2.9. Bonding in poly(ferrocenylenedivinylene)

Tight binding calculations with an extended Hückel Hamiltonian[66,67] were used to provide a qualitative assessment of the bonding in the ferrocenyl polymers and to examine why the poly(ferrocenylenedivinylene) derivatives are rather poor conductors. The parameters used for these calculations are the standard ones in CAESAR[68] and the geometry was adapted from the X-ray structure of **4**.[16] An one-dimensional band model was used for the computations. The density of states (DOS) for the parent poly (ferrocenylenedivinylene) is shown in Figure 10. Here, ε_F indicates the position of the Fermi level. A 1.8 eV gap was found for this polymer. In contrast, the band gap for polyacetylene itself was computed (at the same level) to be 0.7–0.9 eV.[69] In other words, the introduction of a ferrocenyl unit substantially increases the band gap. Consistent with this result is the fact that the band gap in poly(ferrocenylenevinylene) was calculated to be 2.0 eV.

The band structure plot for poly(ferrocenylenedivinylene) is shown on the upper right side of Figure 10. There is some dispersion calculated for the valence and conduction bands, both of which contain substantial butadienyl π character. In other words, the valence band can be identified with the HOMO π orbital of butadiene and the conduction band with the LUMO of butadiene. The coordinate system for poly(ferrocenylenevinylene) is given at the top center of Figure 10. The p_z AOs on carbon are then used for the π-bonding. The dashed line in the DOS plot refers to the projection of carbon p_z for the butadiene linkage. If the ferrocenyl unit were highly conjugating, then the valence band would be more destabilized and the conduction band more stabilized at the zone edge. At the k=X point, the LUMO of butadiene interacts primarily with a higher-lying Cp π combination antibonding to Fe d_{yz}. This interaction stabilizes the conduction band; however, the lower-lying Cp π combination bonding to Fe d_{yz} also mixes into the band and destabilizes it. It is this competition between the two ferrocenyl MOs that keeps the conduction band at high energy for the k=X point. Basically, the same situation applies for the valence band. At k=X, the butadiene HOMO is destabilized by a rather low-lying Cp π combination and stabilized by a Cp π^* MO.

One can also see from both the DOS and band structure plots that the conduction band lies close in energy to a number of states that are highly localized at Fe. These can be associated with the z^2, xy, and x^2-y^2 d AOs of ferrocene.[70] Our calculations are insufficiently accurate to distinguish whether the butadiene π band lies just above or within the highly localized Fe d states. The electrochemical

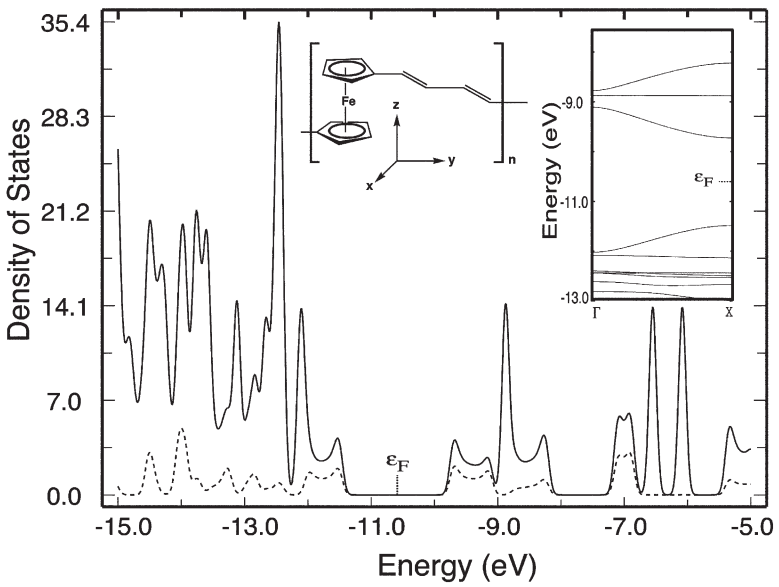

Figure 10. The DOS plot (solid line) for poly(ferrocenylene divinylene). The dashed line indicates the projection of the buadieneyl p_z AOs. The inset on the upper right side show the band structure for this compound around the Fermi level, ε_F.

data presented above would tend to support the latter. Notice, however, that even if the former is true, the density of states at the top of the conduction band is rather low.

An alternative way to view the nature of the bonding is to note that the ferrocenyl unit is 'saturated'. All filled MOs are Cp–Fe bonding and lie at low energies or are highly localized at the metal (note: the z^2, xy and x^2-y^2 d AOs of ferrocene can be viewed as the t_{2g} set of a octahedral complex).[70] The empty MOs are Fe–Cp antibonding or Cp–π^* and are at high energies. A similar situation applies for poly(ferrocenylenevinylene). Because of the parity difference in the HOMO and LUMO of a vinyl group compared to that in a divinyl group, the zone center ($k=\Gamma$) now serves to position the band gap. Putting more unsaturated units between the ferrocenes will decrease the gap, which is consistent with the greater conductivity of doped polyacetylene compared to that of the ferrocenyl-containing polymers. There are two plausible scenarios to generate a smaller band gap. The substitution of π-donors on the unsaturated chains will raise the energy of the valence band. The problem with this strategy is that it should also raise the energy of the conduction band, albeit to a lesser extent. Alternatively if there are an odd number of unsaturated carbon atoms between the ferrocene units, then there will be a non-bonding π level at moderate energies that will interact strongly with the metal. The simplest example would be a fulvene-metal-cyclopentadienyl complex. These compounds have been investigated extensively.[71] Calculations on a poly(ferrocenylenemethylene) model show the presence of a band at moderate energy that lies just above and below the valence and conduction bands in the previous systems.

3. Conclusions

We explored the ring-opening metathesis polymerization of **4** to give organometallic polymer **5** that is fully conjugated and contains repeat units of ferrocene in the polymer backbone. The synthetic strategy outlined here offers a general route to the synthesis of high-molecular weight (e.g. $M_w>300{,}000$) conjugated organometallic polymers that are soluble in common organic solvents. The unprecedented solubility of these compounds permitted the successful characterization of polymer **5**. Analysis by UV/vis spectroscopy revealed bathochromic shifts for polymer **5**, indicating extended conjugation, which is necessary to facilitate electron conduction through the π-conjugated backbone of the polymer. Some degree of electron delocalization through the backbone was also supported by electrochemical measurements, which revealed the presence of two reversible oxidation waves for polymer **5**. The presence of multiple redox waves indicates that the ferrocene nuclei communicate with each other electronically. The similarity of our measured conductivities to those of oligomeric poly(ferrocenylenevinylene)[31] and poly(ferrocenylenebutadiene)[32] suggests that interchain hopping might be the dominant mechanism of transport found in our polymeric system. Incorporation of the *tert*-butyl group lends solubility to polymer **5**, which facilitates the synthesis of high molecular weight materials. The steric bulk of this substituent might, however, play a role in lowering the electric conductivity through various mechanisms. Calculations suggest, however, that the ferrocene group itself is primarily responsible for lowering the conductivity. Future studies will explore the incorporation of alternative side groups and linkages to explore these issues in greater detail.

4. Experimental

4.1. General

Reactions sensitive to air and/or water were performed under an inert atmosphere (N_2 or Ar) using either standard Schlenk techniques or an Innovative Technologies glove box. All bulk polymerizations were performed in the glove box. Hydrocarbon solvents were dried by passage through a column of activated alumina; trace amounts of oxygen were removed with a Cu-based catalyst (Q-5, Englehard). Ethereal and halogenated solvents were dried by passage through a column of activated alumina. All solvents were degassed using freeze-pump-thaw cycles before use. The tungsten-based metathesis initiator, W(=CHC_6H_4-*o*-OMe)(=NPh)[$OCMe(CF_3)_2]_2$ (THF), was prepared as described elsewhere.[39]

4.2. Synthesis and polymerization of 1,1′-(1-*tert*-butyl)-1,3-butadienylene)ferrocene 4

The monomer used in these studies, 1,1′-(1-*tert*-butyl-1,3-butadienylene)ferrocene **4**, was synthesized via the strategy outlined in Scheme 2. The key intermediate, 1,1′-(4-oxo-1-butenylene)ferrocene **9**, was synthesized using methodology developed by Pudelski and Callstrom (see Scheme 2).[53] The procedures for the synthesis and polymerization of 1,1′-(1-*tert*-butyl-1,3-butadienylene) ferrocene **4** have been described in detail in our previous report.[16] Complete analytical data were previously reported for the monomer **4** and the polymer **5**.[16]

4.3. Nuclear magnetic resonance (NMR) spectroscopy

NMR spectra were recorded with a General Electric QE-300 (300.2 MHz, ^1H; 75.5 MHz, ^{13}C) spectrometer equipped with a dual probe. Data were collected as indicated in either benzene-d_6, methylene chloride-d_2, or chloroform-*d*. Chemical shifts were referenced to the residual proton or carbon signal of the deuterated solvents.

4.4. Ultraviolet–visible (UV–vis) absorption spectroscopy

Ultraviolet–visible absorption spectra were collected on a Varian Cary 3-Bio UV–visible spectrophotometer. The compounds were dissolved in THF or CH_2Cl_2, and the data were collected over the range of 300–600 nm in a standard quartz cell 1×1×4 cm^3.

4.5. Thermal gravimetric analysis (TGA)

The thermal degradation of polymer **5** was evaluated using a TA Instrument Hi-Res TGA 2950 Thermogravimetric Analyzer. An aliquot of the polymer sample (~12 mg)

was heated at 0.5 °C/min under a flow of N_2 gas. The percent weight loss of the sample vs. temperature was recorded.

4.6. Differential scanning calorimetry (DSC)

DSC data were collected using a TA Instrument DSC 2010 in a sealed aluminum pan. The sample was heated from 50 to 250 °C at a rate of 10 °C/min under a flow of nitrogen. Conventional heat flow vs. temperature was obtained using a Universal V2.5H TA Instruments program.

4.7. Gel permeation chromatography (GPC)

GPC was used to determine the molecular weights of polymer samples. The GPC system consisted of a Waters 510 pump and a Waters 410 differential refractive index detector. The column set included three Waters Styragel HR columns (Styragel HR 5E, 4E, and 1 in series). THF was used as the eluant, and the flow rate was 1.0 mL/min. The column set was calibrated with narrow molecular weight polystyrene standards purchased from Polysciences. The polymer samples (3–5 mg mL^{-1}) were filtered through a 0.45 μm Millipore, Millex FH 13 mm filter prior to analysis.

4.8. Spin-casting and doping of thin polymer films

A sample of polymer (20 mg) was dissolved in benzene (1 mL) and filtered through a 0.45 μm Millipore, Millex FH 13 mm filter. The solution was cast dropwise onto a glass substrate mounted on Headway Research Spin-Coater. The translucent red films were spun dry and then further dried under vacuum. Doping was accomplished by exposing the polymer films to iodine vapor (200 mm Hg) in an evacuated Schlenk flask for selected intervals of time (typically 2–5 h). The initially translucent red films became black upon exposure to iodine. Before measuring the conductivity, the sample was placed under vacuum for ~30 min to remove any excess iodine.

4.9. Measurements of electrical conductivity

In order to eliminate contact resistance, the conductivities were measured using the four-point probe method.[11,14] Our homemade four-point probe system consists of four-in-line heads (Keithley), an autoranging digital multimeter (Kiethley Model 2001), a picoammeter (Kiethley Model 487), and software programmed to measure the voltage and resistivity of the sample (Keithley TestPoint). Four thin gold wires (0.05 mm thick and 99.9% pure) were attached in parallel on the film surface with colloidal silver liquid (Ted Pella, Inc.) for enhanced electrode contact. Conductivity values (σ) were obtained by connecting the four probes to four gold wires on the surface of the doped film, applying a potential via the power source, and measuring the resulting current (i) and the voltage drop (v) between the four probes.

The conductivities were calculated according to the van der Pauw Eq. (1), which applies for a sample in which the thickness (d) is less than the probe spacing. The values of conductivity reported in the text were obtained from the average of a series of multiple current and voltage measurements. To confirm the accuracy of the detection circuit, measurements were performed on standard resistors prior to collecting the data on the doped samples.

$$\sigma = \mathrm{i}(\ln 2)/(\pi dv) \quad (1)$$

Using the apparatus, the electrical conductivities of the polymer samples were measured in an inert atmosphere or in air. Inert atmosphere measurements were performed in a glove box or in Schlenk reaction vessels sealed with rubber septa. Conductivity measurements in air of doped films gave sporadic data, representative of oxidative degradation of the conducting films. Therefore, the reported conductivities of all doped material were collected under an inert atmosphere. Measurements in air were only performed for undoped samples, which were found to be stable in air.

Acknowledgements

Generous support for this research was provided by the Robert A. Welch Foundation (Grants E-0705 and E-1320) and the Texas Institute for Intelligent Bio-Nano Materials and Structures for Aerospace Vehicles, funded by NASA Cooperative Agreement No. NCC-1-02038.

References and notes

1. Arimoto, F. S.; Haven, A. C., Jr. *J. Am. Chem. Soc.* **1955**, *77*, 6295.
2. Chen, Y.-H.; Fernandez-Refojo, M.; Cassidy, H. G. *J. Polym. Sci.* **1959**, *40*, 433.
3. Pittman, C. U., Jr.; Lai, J. C.; Vanderpool, D. P.; Good, M.; Prado, R. *Macromolecules* **1970**, *3*, 746.
4. Cowan, D. O.; Park, J.; Pittman, C. U., Jr.; Sasaki, Y.; Mukherjee, T. K.; Diamond, N. A. *J. Am. Chem. Soc.* **1972**, *94*, 5110.
5. Pittman, C. U., Jr.; Sasaki, Y.; Grube, P. L. *J. Macromol. Sci.-Chem.* **1974**, *A8*, 923.
6. Marks, T. J. *Science* **1985**, *227*, 881.
7. *Handbook of Conducting Polymers*, Skotheim, T. A., Ed.; Marcel Dekker: New York, 1986; Vols. 1 and 2.
8. Sailor, M. J.; Ginsberg, E. J.; Gorman, C. B.; Kumar, A.; Grubbs, R. H.; Lewis, N. S. *Science* **1990**, *249*, 1146.
9. Allcock, H. R. *Science* **1992**, *3*, 381.
10. Bunz, U. H. F. *Angew. Chem., Int. Ed. Engl.* **1996**, *35*, 969.
11. Much recent interest has focused on a family of non-π-conjugated polymers that contain ferrocenylene units in the backbones. See, for example: Manners, I. *Angew. Chem., Int. Ed. Engl.* **1996**, *35*, 1602. and Pannell, K. H.; Dementiev, V. V.; Li, H.; Cervantes-Lee, F.; Nguyen, M. T.; Diaz, A. F. *Organometallics* **1994**, *13*, 3644.
12. Brizius, G.; Pschirer, N. G.; Steffen, W.; Stitzer, K.; zur Loye, H.-C.; Bunz, U. H. F. *J. Am. Chem. Soc.* **2000**, *122*, 12435.
13. Morisaki, Y.; Chujo, Y. *Macromolecules* **2003**, *36*, 9319.
14. For reviews, see: Nguyen, P.; Gomez-Elipe, P.; Manners, I. *Chem. Rev.* **1999**, *99*, 1515.
15. For reviews of inorganic and organometallic polymers, see: Mark, J. E.; Allcock, H. R.; West, R. *Inorganic Polymers*. Prentice Hall: New Jersey, 1992. *Inorganic and Organometallic Polymers II*; *ACS Symposium Series 572*, Wisian-Neilson, P., Allcock, H. R., Wynne, K. J., Eds.; American Chemical Society: Washington, DC, 1994.

16. Heo, R. W.; Somoza, F. B.; Lee, T. R. *J. Am. Chem. Soc.* **1998**, *120*, 1621.
17. Heo, R. W.; Lee, T. R. *Polym. Prepr.* **1998**, *39*, 169.
18. Gooding, R.; Lillya, C. P.; Chien, J. C. W. *J. Chem. Soc., Chem. Commun.* **1983**, 151.
19. Scholl, H.; Sochaj, K. *Electrochim. Acta* **1991**, *36*, 689.
20. Cotton, F. A.; Wilkinson, G. *Basic Inorganic Chemistry*; Wiley: New York, 1987; p 622.
21. Osborne, A. G.; Whiteley, R. H.; Meads, R. E. *J. Organomet. Chem.* **1980**, *193*, 345.
22. Butler, I. R.; Cullen, W. R.; Einstein, F. W. B.; Rettig, S. J.; Willis, A. J. *Organometallics* **1983**, *2*, 128.
23. Herberhold, M. *Angew. Chem., Int. Ed. Engl.* **1995**, *34*, 1837.
24. Manners, I. *Adv. Organomet. Chem.* **1995**, *37*, 131.
25. Berenbaum, A.; Braunschweigh, H.; Dirk, R.; Englert, U.; Green, J. C.; Jakle, F.; Lough, A. J.; Manners, I. *J. Am. Chem. Soc.* **2000**, *122*, 5765.
26. Temple, K.; Dziadek, S.; Manners, I. *Organometallics* **2002**, *21*, 4377.
27. Berenbaum, A.; Lough, A. J.; Manners, I. *Organometallics* **2002**, *21*, 4415.
28. Foucher, D. A.; Tang, B. Z.; Manners, I. *J. Am. Chem. Soc.* **1992**, *114*, 6246.
29. Naarmann, H.; Theophilou, N. *Synth. Met.* **1987**, *22*, 1.
30. Murase, I.; Ohnishi, T.; Noguchi, T.; Hirooka, M. *Polym. Commun.* **1994**, *25*, 327.
31. Buretea, M. A.; Tilley, T. D. *Organometallics* **1997**, *16*, 1507.
32. Stanton, C. E.; Lee, T. R.; Grubbs, R. H.; Lewis, N. S.; Pudelski, J. K.; Callstrom, M. R.; Erickson, M. S.; McLaughlin, M. L. *Macromolecules* **1995**, *28*, 8713.
33. Itoh, T.; Saitoh, H.; Iwatsuki, S. *J. Polym. Sci., Polym. Chem.* **1995**, *33*, 1589.
34. Knapp, R.; Velten, U.; Rehahn, M. *Polymer* **1998**, *39*, 5827.
35. Bochmann, M.; Lu, J.; Cannon, R. D. *J. Organomet. Chem.* **1996**, *518*, 97.
36. Ingham, S. L.; Khan, M. S.; Lewis, J.; Long, N. J.; Raithby, P. R. *J. Organomet. Chem.* **1994**, *470*, 153.
37. Buchmeiser, M. R.; Schuler, N.; Kaltenhauser, G.; Ongania, K. H.; Lagoja, I.; Wurst, K.; Schottenberger, H. *Macromolecules* **1998**, *31*, 3175.
38. Schrock, R. R.; Murdzek, J. S.; Bazan, G. C.; Robbins, J.; DiMare, M. R. *J. Am. Chem. Soc.* **1990**, *112*, 3875.
39. Gorman, C. B.; Ginsburg, E. J.; Grubbs, R. H. *J. Am. Chem. Soc.* **1993**, *115*, 1397, and references therein.
40. Hotta, S.; Rughooputh, S. D. D. V.; Heeger, A. J.; Wudl, F. *Macromolecules* **1987**, *20*, 212.
41. MacIness, D., Jr.; Funt, B. L. *Synth. Met.* **1988**, *25*, 235.
42. Elsenbaumer, R. L.; Jen, K.; Miller, G. G.; Eckhardt, H.; Shacklette, L. W.; Jow, R. *Electronic Properties of Conjugated Polymer*; Kuzmany, H., Mehhring, M., Roth, S., Eds.; Springer: Berlin, 1987; Vol. 76, pp 400–406.
43. Rehahn, M.; Schluter, A. D.; Wegner, G.; Feast, W. J. *Polymer* **1989**, *30*, 1060.
44. Havinga, E. E.; van Korssen, L. W. *Polym. Bull.* **1988**, *18*, 2777.
45. Grubbs, R. H.; Tumas, W. *Science* **1989**, *243*, 907.
46. Schrock, R. R. *Acc. Chem. Res.* **1990**, *23*, 158.
47. Gilliom, L. R.; Grubbs, R. H. *J. Am. Chem. Soc.* **1986**, *108*, 733.
48. Novak, B. M.; Grubbs, R. H. *J. Am. Chem. Soc.* **1988**, *110*, 7542.
49. Cannizzo, L. F.; Grubbs, R. H. *Macromolecules* **1988**, *21*, 1961.
50. Risse, W.; Wheeler, D. R.; Cannizzo, L. F.; Grubbs, R. H. *Macromolecules* **1989**, *22*, 3205.
51. Johnson, L. K.; Virgil, S. C.; Grubbs, R. H.; Ziller, J. W. *J. Am. Chem. Soc.* **1990**, *112*, 5384.
52. Pudelski, J. K.; Callstrom, M. R. *Organometallics* **1992**, *11*, 2757.
53. Pudelski, J. K.; Callstrom, M. R. *Organometallics* **1994**, *13*, 3095.
54. March, J. *Advanced Organic Chemistry*; Wiley: New York, 1992; Chapter 17.
55. Erickson, M. S.; Fronczek, F. R.; McLaughlin, M. L. *Tetrahedron Lett.* **1992**, *2*, 197.
56. Odian, G. *Principles of Polymerization*; Wiley: New York, 1991.
57. Similar steric constraints have been observed in ring-closing metathesis (RCM) reactions: Kirkland, T. A.; Grubbs, R. H. *J. Org. Chem.* **1997**, *62*, 7310.
58. Scott, A. I. *Interpretation of the Ultra–violet Spectra of Natural Products*; MacMillan: New York, 1964.
59. Mohammad, F. Degradation and Stability of Conductive Polymers. In: *Handbook of Organic Conductive Molecules and Polymers*; Wiley: New York; 1996, Vol. 3, Chapter 16.
60. Ito, T.; Shirakawa, H.; Ikeda, S. *J. Polym. Sci. Chem.* **1975**, *13*, 1943.
61. Kovacic, P.; Kyriakis, A. *J. Am. Chem. Soc.* **1963**, *85*, 454.
62. Nguyen, M. T.; Diaz, A. F.; Dement'ev, V. V.; Pannell, K. H. *Chem. Mater.* **1993**, *5*, 1389.
63. Nguyen, M. T.; Diaz, A. F.; Dement'ev, V. V.; Pannell, K. H. *Chem. Mater.* **1994**, *6*, 952.
64. Flanagan, J. B.; Margel, S.; Bard, A. J.; Anson, F. C. *J. Am. Chem. Soc.* **1978**, *100*, 4248.
65. Nelson, J. M.; Rengel, H.; Manners, I. *J. Am. Chem. Soc.* **1993**, *115*, 7035.
66. Hoffmann, R. *J. Chem. Phys.* **1963**, *39*, 1397.
67. Whangbo, M.-H.; Hoffmann, R. *J. Am. Chem. Soc.* **1978**, *100*, 6093.
68. Whangbo, M.-H.; Ren, J.; Weigen, L. *CAESAR*; North Carolina State University: Raleigh, 1998.
69. Whangbo, M.-H.; Hoffmann, R.; Woodward, R. B. *Proc. R. Soc. London A* **1979**, *366*, 23.
70. Albright, T. A.; Burdett, J. K.; Whangbo, M. H. *Orbital Interactions in Chemistry*; Wiley: New York, 1985.
71. See for example, Barlow, S.; Cowley, A.; Green, J. C.; Brunker, T. J.; Hascall, T. *Organometallics* **2001**, *20*, 5351, and references therein.